Influence of Electrical Steel Grade on Different Types of Traction Motors

X. Y. Ma, J. Soulard, C. Slater, and C. Davis

Abstract –**This paper provides a systematic approach to study the influence of electrical steel grade on electric vehicle traction motor performance. A permanent magnet assisted synchronous reluctance motor, an interior permanent magnet motor and an induction motor are considered to systematically quantify the influence of lamination thicknesses from 0.1 to 0.35mm, and materials with 3% and 6.5% silicon contents. Laminations with low silicon steel are better candidates in terms of peak and continuous torque production for low-speed operations. 0.1mm 6.5% silicon steel - 10JNEX900 can achieve higher efficiency and better flux-weakening capability above 400 Hz. Its higher mechanical strength is beneficial for complex rotor structure with bridges under stress from centrifugal forces. Therefore, grade choice relies on a compromise between low and high speed performance, propulsion system cost estimation and manufacturing challenges. Application related priorities define which grade is best suited.**

Index Terms— **Electrical steel, iron loss, permanent magnet motor, induction motor, synchronous reluctance motor, propulsion.**

I. INTRODUCTION

As the core component of electric vehicle (EV) propulsion system, traction motors normally require high torque density, high power density, wide constant power speed range, high efficiency, high reliability, low vibration and acoustic noise at acceptable cost and manufacturing challenges. [1] [2].

Among various types of electrical machines (e-machines), interior permanent magnet machines (IPMs) and induction machines (IMs) are two promising candidates for traction system. However, the drawbacks of an IPM could be the relatively high cost and the risk of irreversible demagnetization of the permanent magnet (PM) [1]. An IM with no rare-earth material can have relatively low cost but a provides lower efficiency compared with an IPM at low speeds. For commercial applications, IPM is adopted in Toyota Prius and Nissan Leaf. IM is utilized in Tesla model S. BWM i3 uses PM assisted synchronous reluctance machine (PMa-SynRM), which is also a competitive candidate, with the merits of less PM usage keeping high torque density due to additional reluctance torque [3], [4]. Accordingly, these three different types of traction motors have been selected for this paper.

Designers of traction motors are looking towards higher speed/frequency to raise power density combined with low cost of material, i.e., value for money is important during the steel grade selection. To reduce losses, either thinner laminations or higher silicon contents keep eddy currents under control [5]. Thinner lamination will lead to higher material and manufacturing costs due to more laminations to be stamped and assembled. In recent years, further binary-based silicon steel (Si-Fe) alloys have been produced in the laboratory with a commercially available 6.5% Si-Fe offering superior properties such as high electrical resistivity, reduced magnetostriction and moderate saturation magnetization [6]. The reduction of eddy current losses makes it attractive for high-speed motor applications [7]. However, this steel is difficult to process in conventional steel plants due to its low ductility, requiring an expensive vapour deposition or heat treatment process to diffuse silicon into the strip. The resultant material is inherently brittle making it more challenging to manufacture into laminations than 3% Si-Fe [5], with increased demands on punching tools. Consequently, it is important to identify and quantify the advantages and drawbacks of thinner lamination or higher silicon contents in terms of improved performance and manufacturing requirements.

The influence of electrical steel (e-steel) grades on motor performances has been investigated in [7] and [8] for surface-mounted PM machines (SPMs) in aircraft generators. In [7], lower iron loss is obtained with 6.5% Si-Fe lamination compared to 3% Si-Fe. Cobalt iron (Co-Fe) is also an alternative for high power density e-machines in aerospace and defence application [9]. This is mainly because the high saturation flux density may lead to weight minimization. But it is the most expensive of the e-steel material considered here. In [8], 6.5% Si-Fe lamination presented merits with lower weight and lower losses than Co-Fe. In addition, the iron loss increase in 6.5% Si-Fe is about 10% lower than Co-Fe under the variation from 50% to 125% of the saturation flux density. With experimental validation in [10], the acoustic noise of a switched reluctance motor with 6.5% Si-Fe lamination is 5% lower than with amorphous iron at 3000 rpm.

For a comprehensive investigation using simulation only of e-steel grades influence on traction motor performance, conventional e-steel (Silicon content less than 3%), as well as 6.5% Si-Fe and thicknesses from 0.1 mm to 0.35mm are considered. The comparison includes systematic electromagnetic, thermal as well as mechanical performance simulations, to derive guidelines

This work was supported in part by the EPSRC FEMM Hub under a feasibility grant (EP/S018034/1).

Dr Xi-Yun Ma, Dr Juliette Soulard, Dr Carl Slater and Prof Claire Davis are with the Warwick Manufacturing Group, University of Warwick, Coventry, U.K. (e-mails: xiyun.ma@warwick.ac.uk, j.soulard@warwick.ac.uk, c.d.slater@warwick.ac.uk, claire.davis@warwick.ac.uk)

for promising materials to be considered at design stage.

TABLE I
TYPICAL ELECTRICAL STEEL MATERIALS FOR E-MACHINES

	Thickness (mm)	Resistivity (μΩm)	Density (kg/m3)	Iron loss at 1.5 T, 50Hz (W/kg)	Flux density at 10 kA/m (T)
M400-50A	0.5	0.42	7650	3.4	1.8
M235-35A	0.35	0.59	7650	2.3	1.8
NO10	0.1	0.52	7650	3.2	1.7
NO20	0.2	0.52	7650	2.4	1.7
CoFe	0.2	0.44	8120	1.6	2.3
10JNEX900	0.1	0.82	7490	1.4	1.7

II. ELECTRICAL STEEL PROPERTIES

A. Typical e-steel materials for electrical motors and their properties

Typical e-steel properties have been listed in Table I in terms of thickness, resistivity, and density. Iron loss density is significantly influenced by material properties in terms of grain size, impurities, texture, silicon content and sheet thickness [6]. Lower hysteresis loss can be obtained by larger grain size, but it is likely to yield more eddy current loss. Impurities such as silicon content leads to higher hysteresis loss and reduced saturation flux density [11].

$$P_{eddy}\ (W/kg) = \frac{\pi^2 (Lamination\ thickness)^2}{6 \times density \times resistivity} f^2 B^2 \qquad (1)$$

Based on Bertotti's iron loss model [12], the eddy current loss density equation in (1) allows to rapidly assess impact of both reduced thickness and higher resistivity on e-machine iron losses, while assuming the flux density pattern is not influenced (similar BH curves for the materials to be compared) and when the frequency is high enough so that the eddy currents are the main contributor to the total losses.

Fig. 1 provides the information to compare the materials' an-hysteretic BH curve at low frequency used for the FEA simulations at all speeds, together with the PB2 value depicted by the size of the disks. PB2 is the ratio of the iron loss density by the squared flux density. This quantity enables to have a visual representation of the iron loss density at given flux density and frequency [5]. If the disk size is constant on a graph at given frequency, it means the losses are dominated by eddy currents, while the hysteresis loss is predominant if the disk size reduces with the flux density level.

Cobalt iron is the most expensive alloy due to its high Cobalt content of 49%. However, the size and weight of motors with Co-Fe can be decreased due to the higher saturation flux density [13]. It is added in the comparison since the proposed method for material selection is usable for aerospace applications too, where this material is highly utilised. Co-Fe has the next to lowest iron loss density at 50Hz, 1.5T but has higher loss than NO10 at 1kHz. For conventional (lower or equal to 3%) Si-Fe, M235-35A has the highest resistivity, while NO10 and NO20 have a smaller lamination thickness with 0.1 mm and 0.2mm, respectively.

Higher silicon content significantly increases resistivity of the e-steel [14]. At 50 Hz, the specific iron loss of 6.5% Si-Fe (10JNEX900) is only 25% compared to M235-35A under the same magnetic field. The difference is higher at 1kHz. However, lower saturation flux density of 6.5% Si-Fe will have an impact too on the motor performance. While with a higher saturation flux density and moderate iron loss density, NO10 possibly provides an interesting solution, since with the 0.1mm thick part, punching and assembly could be challenging.

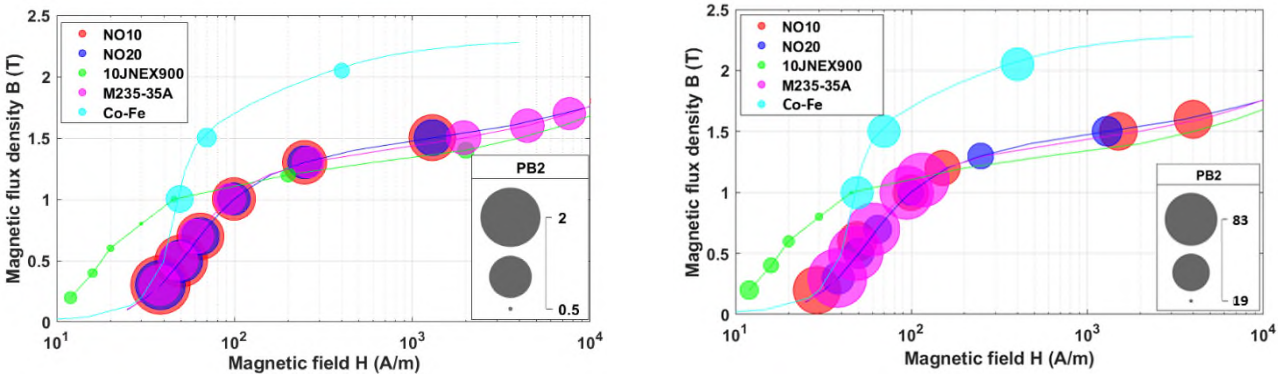

Fig. 1 E-steel material anhysteretic BH curve with iron loss to squared flux density values (PB2) at different frequencies. (a) 50 Hz. (b) 1000 Hz.

B. Mechanical properties

Yield stress of lamination material impacts the design of the rotor. Bridges in buried magnets configurations are subjected to high local stress by centrifugal forces, worst case being at over-speed (120% of maximum speed). Fig. 2 presents the yield stress

as function of core-loss densities for commercial e-steel grades at 50Hz and 1 kHz, respectively. The Co-Fe with 0.2 mm thickness has the lowest yield stress. Consequently, it is a challenge to use in rotors with buried magnets for high-speed applications. For 3% Si-Fe, M235-35A with 0.35 mm thickness has a yield stress around 460 MPa. NO10 and NO20 have lower yield stress than M235-35A but have been qualified as the cost-effective alternatives for high volume manufactured motors with lower core losses [15]. The hardness of material increases with increasing silicon content in the steel since silicon strengthens the solid solution [16]. Thus, the 6.5% Si-Fe (10JNEX900) has the highest yield stress of the considered materials with 600MPa.

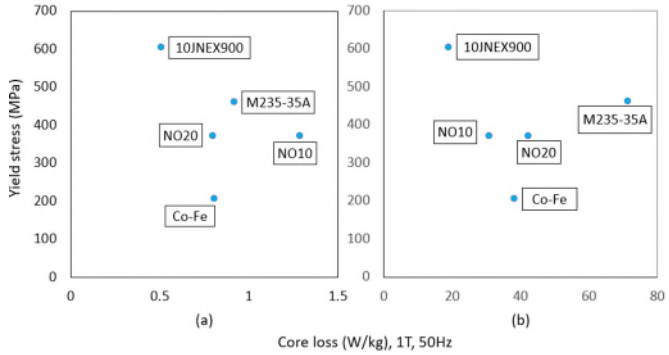

Fig. 2 Yield stress and core loss characteristics for commercial e-steel grades at different frequency. (a) 50 Hz, (b) 1000 Hz.

III. ELECTRICAL MOTORS FOR TRACTION SYSTEM

Three different types of electrical motors for traction system have been investigated in this paper. They are the interior PM motor (IPM) from Nissan Leaf [17], induction motor (IM) from Tesla model S [17], and a PM assisted synchronous reluctance motor (PMa-SynRM) for FreedomCar 2020 application [18]. Fig. 3 shows the cross-section view of the motors.

A. Interior PM motor (IPM)

Nissan Leaf traction motor is a 3-phase, 48-slot/8-pole IPM with distributed winding, as shown in Fig. 3(a). With the magnets buried inside the rotor, the IPM has the potential to achieve a wide speed range of constant power. This rotor consists of 2 layers of magnets: flat and V-shape, which has the advantage of additional reluctance torque and thus, higher torque density. With a stator outer diameter of 198 mm and axial length of 150 mm, the motor peak torque is 266 N.m and the peak power is 129kW. The base speed of the IPM is 4000 rpm (267 Hz), and its maximum speed is 10000 rpm (667 Hz).

B. PM assisted synchronous reluctance motor (PMa-SynRM)

The synchronous reluctance motor (SynRM) with insertion of a PM in one of the rotor flux barriers (PM-assisted) has a higher torque and power factor than the pure SynRM. Fig. 3(b) is a 3-phase, 30-slot/10-pole motor designed for FreedomCar 2020 application [18]. Distributed winding is employed to generate more reluctance torque than fractional-slot winding. [4]. With a stator outer diameter of 250 mm and axial length of 100 mm, the peak performance of the PMa-SynRM is 200 N.m and 55 kW. The electrical frequencies at base speed 2800 rpm and maximum speed 14000 rpm are 233 Hz and 1167 Hz, respectively.

C. Induction motor (IM)

The IM is employed in Tesla model S traction system. It has 72 stator slots and 84 rotor bars (see Fig. 3(c)). The rotor has 6 poles with a copper cage. With an outer diameter of 250 mm and an axial length of 120 mm, the peak torque and peak power of the IM are 390 N.m and 324 kW, respectively. The electrical frequencies are 328 Hz at base speed of 6500 rpm and 747 Hz at maximum speed of 14800 rpm.

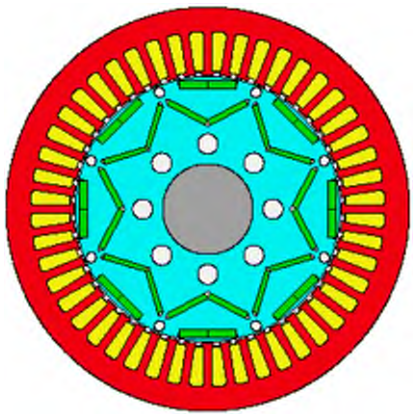

(a)

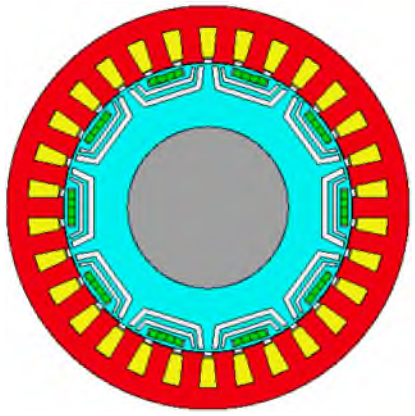

(b)

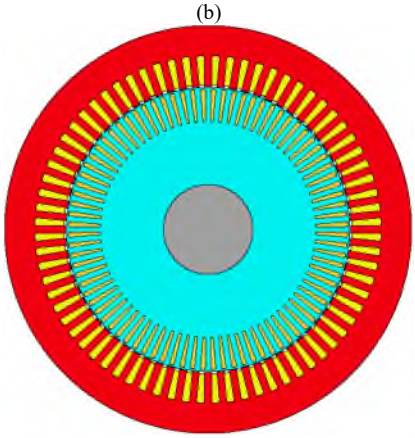

(c)

Fig. 3 Cross-sections of different traction motors. (a) IPM, (b) PMa-SynRM, and (c) IM.

IV. Influence of E-steel Materials on Motor Performances

E-machine performance are calculated and compared systematically for typical e-steel grades including conventional Si-Fe (M235-35A), 3% Si-Fe (NO10) and 6.5% Si-Fe (10JNEX900) in each motor in Section III. Mid-grade like NO20 was not included because the influence is rather small compared to NO10.

The influence of e-steel grades on local flux densities, torque, iron losses, peak torque speed characteristics and efficiency map is quantified. In addition, thermal performance evaluation has been conducted via continuous thermal envelope, in which the winding and magnet temperatures are kept within their maximum limits. Moreover, mechanical stress and rotor radial displacement have been analysed at a 20% over the rotor maximum speed.

A. Flux density

The difference in BH curves of e-steel grades leads to some changes in local flux densities. Fig. 4 compares the average airgap flux density, peak stator tooth flux density, and peak stator back iron flux density of the three motors that vary only by a few % at maximum inverter current and at respective base speeds.

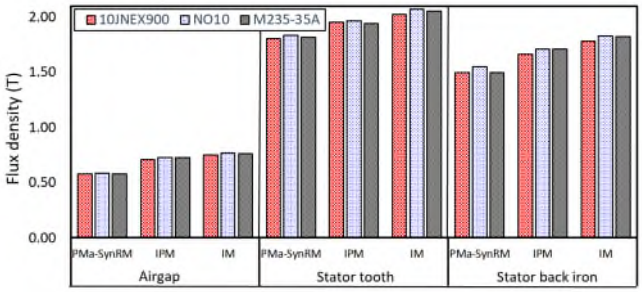

Fig. 4 Local flux densities at motor peak performance. PMa-SynRM: 370A and 2800rpm (233Hz). IPM: 480A and 4000rpm (267Hz). IM: 900A and 6500 rpm (328Hz).

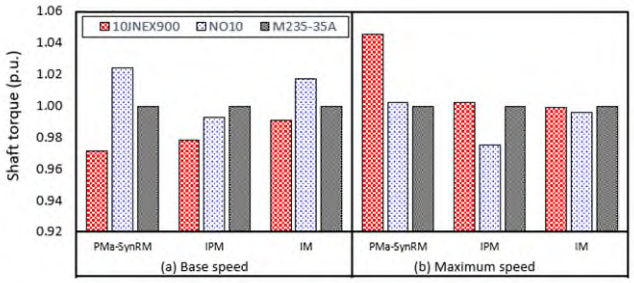

Fig. 5 Comparison of torque-speed characteristics in terms of two operating points. (a) rotor base speed, (b) maximum speed.

The three motors have been designed at different levels of saturation, which can be seen from the flux densities in stator tooth and stator back iron. At motor peak performance, the IM is at the highest saturation level followed by the IPM. The difference in airgap flux density due to e-steel grades are very small. Regardless of motor types, the lowest airgap flux density is with 10JNEX900 lamination due to its lower magnetic saturation above 1.2T. For e-steels with low silicon content, a slightly higher airgap flux density can be achieved with NO10 lamination in PMa-SynRM (0.7%) and IM (0.4%). It is slightly higher with M235-35A in the IPM but only marginally 0.2%. The comparison is only valid for the respective base working points of the three motors.

B. Peak torque-speed characteristics

Peak torque-speed characteristics have been evaluated under the limitation of inverter maximum current and DC bus voltage, without thermal consideration. Two operating points on the torque-speed curve have been selected for the comparison, as shown in Fig. 5. One is at the rotor base speed and the other is at the maximum speed. For a better visualization of the torque comparison, a normalization is used with the torque produced with M235-35A lamination as reference (1p.u), which would be the most likely material due to its reduced cost compared to the other two grades.

Compared to the reference grade M235-35A, a higher torque can be obtained with thinner lamination grade, i.e., NO10, for both PMa-SynRM and IM. For the IPM design, M235-35A lamination gives the highest peak torque value. With higher silicon content and thinner thickness, 10JNEX900 does not show any advantages in terms of torque at rotor base speed (<350 Hz), with reduced torque values by less than 5% compared to other grades. At rotor maximum speed, the fundamental frequency is increased to 1167 Hz, 667 Hz, 747 Hz in the PMa-SynRM, IPM and IM, respectively. As can be seen from Fig. 5(b), using 10JNEX900 lamination gives highest torque for each of the three motors. Particularly a 5% higher torque is calculated for the PMa-SynRM, which operates at the highest frequency among the three motors.

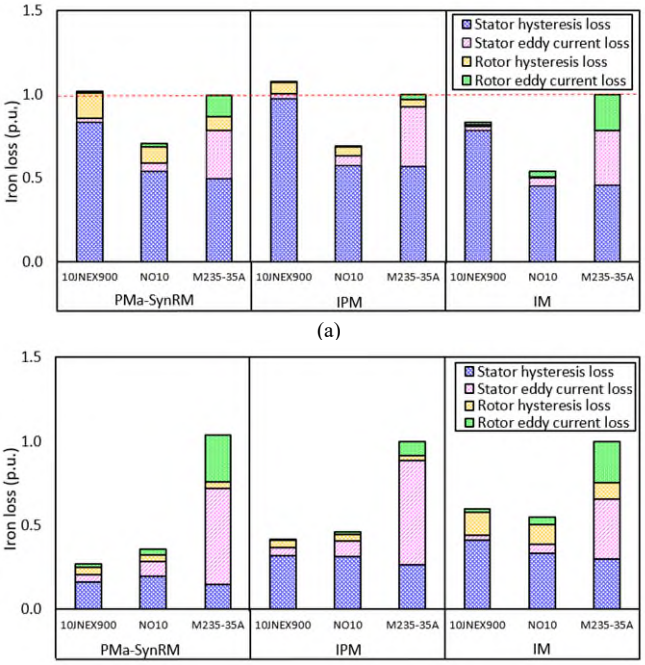

Fig. 6 Comparison of iron losses at two operating points on torque-speed curves. (a) rotor base speed and (b) maximum speed.

C. Iron losses

Copper losses and iron losses are the two main loss components of a motor in propulsion systems. At high current and low speed range, copper loss is dominating since it is directly proportional to square of phase current. While at high-speed range, iron losses are a substantial contributor to the total loss. Using the Steinmetz loss model, iron losses have been simulated at both rotor base speed and rotor maximum speed. Fig. 6 summarizes iron losses with the split in terms of hysteresis and eddy current losses in both stator and rotor, with per-unit values defined by losses for the M235-35A total iron loss.

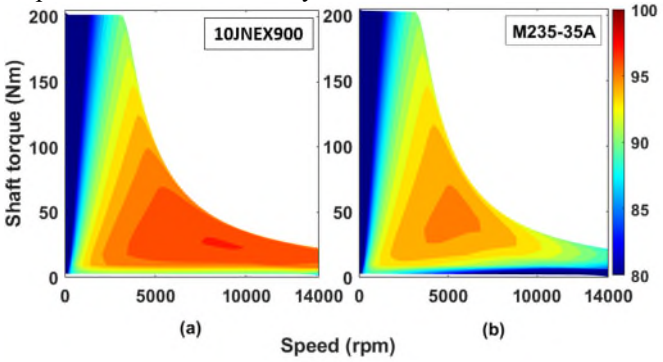

Fig. 7 Efficiency map of PMa-SynRM. Maximum efficiency is 97% with 10JNEX900 and 95% with M235-35A.

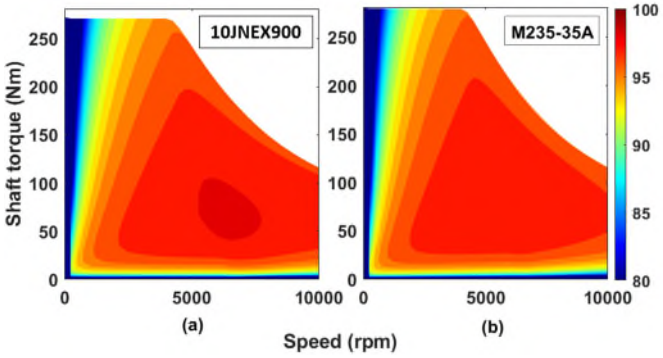

Fig. 8 Efficiency map of IPM. Maximum efficiency is 98% with 10JNEX900 and 97% with M235-35A.

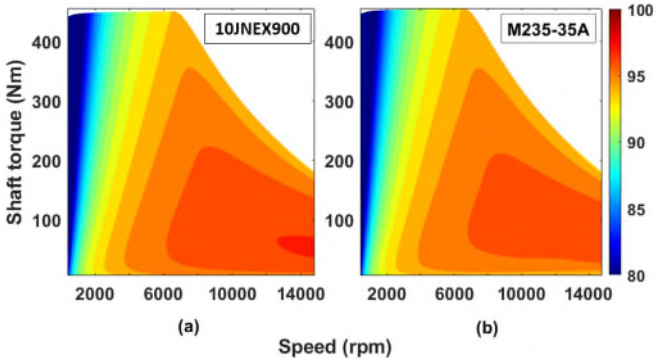

Fig. 9 Efficiency map of IM. Maximum efficiency is 97% with 10JNEX900 and 96% with M235-35A.

Thanks to thinner lamination and higher resistivity, 10JNEX900 creates the lowest eddy current loss, which is about 12 times lower than M235-35A at both low and high frequencies for all motors. However, hysteresis loss is the dominant part of total iron losses at low frequency (lower than 400Hz). More than 85% of the total iron losses for 0.1 mm thickness (NO10 and 10JNEX900) and 46% for M235-35A are hysteresis losses. In addition, 10JNEX900 generates about 41% higher hysteresis loss than M235-35A. Consequently, benefit of lower eddy current loss in 10JNEX900 is counteracted by its higher hysteresis loss. With about the same level of low hysteresis loss as M235-35A and slightly higher eddy current loss than 10JNEX900 due to lower resistivity, NO10 gives the lowest iron losses at peak torque and low frequency.

At rotor maximum speed (higher than 400Hz), hysteresis loss is still the dominant part in laminations with 0.1 mm thickness (NO10 and 10JNEX900). While with M235-35A, motor eddy current loss increases drastically and becomes the dominant part of the iron losses. As a result, M235-35A is the worst choice for high frequency application in terms of iron losses for all motors. By way of example, the iron losses can be reduced by 73% with 10JNEX900 and 63% with NO10 in a PMa-SynRM, compared to M235-35A.

D. Efficiency map

E-steel material is expected to have impact on the motor efficiency map due to the difference in torque-speed characteristics and iron losses. Fig. 7, Fig. 8, and Fig. 9 illustrate the efficiency map of the PMa-SynRM, IPM, and IM with 10JNEX0900 and M235-35A laminations, respectively. The maximum motor efficiency can be attained by 10JNEX900 lamination. The difference is insignificant when comparing the motors with NO10 and 10JNE9000 laminations so efficiency maps with NO10 are not shown in the figures.

10JNEX900 produces 2% higher efficiency compared with M235-35A in the PMa-SynRM at its highest point. The region with efficiency higher than 95% covers the speed range from 1600 rpm to 14000 rpm. For M235-35A, the same region is only between 3800 rpm and 6800 rpm. As a result, the PMa-SynRM with 10JNEX900 can operate at a higher efficiency and a wider speed range. The benefit of 10JNEX900 in efficiency map can also be seen in the IPM and IM but it is not as obvious. It may be because of the IPM relies more on permanent magnet, not the e-steel. In the IM, copper loss and rotor cage loss tend to dominate the total iron losses, hence, benefit of the iron losses with 10JNEX900 lamination is only visible above 7000 rpm.

E. Continuous torque envelope

For the peak torque-speed characteristics, machine cooling is not considered. For continuous performance simulation, maximum allowed temperature of the winding hotspot is set to 160℃, magnets for the IPM and PMa-SynRM are limited to 140℃, winding combined with rotor laminations temperature for the IM is limited to 200℃. The inverter current is reduced to reach either of the temperature limits, defining the maximum torque at thermal steady-state i.e. the continuous torque-speed envelope.

The three motors were assigned a similar water jacket cooling system and EGW50/50 was selected as the coolant. Continuous torque-speed and power-speed envelopes are compared among different e-steel grades in Fig. 10. At low-speed range, motor performance is limited by the stator winding temperature. The highest torque is obtained with NO10 for the PMa-SynRM, while M235-35A is best in the IPM and IM. Magnet temperature is the limiting factor at high-speeds for PM motors while the stator winding temperature limits the IM performance. The best torque and power capability is achieved with 10JNEX900 when the fundamental frequency is higher than around 400 Hz for all motors. It can be concluded that 10JNEX900 enhances power capability at high frequency for the 3 types of motors considered.

F. Mechanical performance at over speed condition

Mechanical performance is important to be considered in motor designs, particularly for high-speed motors. 10JNEX900 manufactured has the highest yield stress among the considered grades, with NO10 showing the lowest value, -39% compared to 10JNEX900.

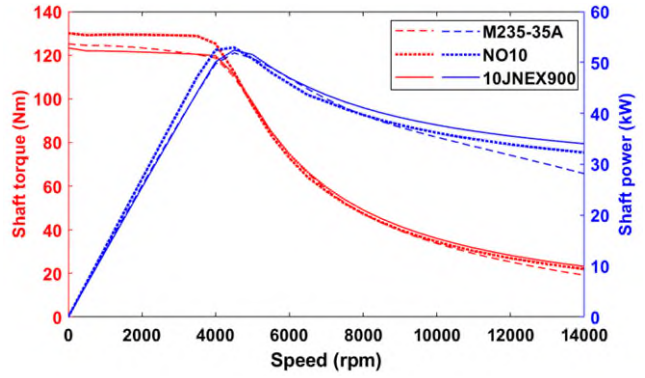

(a)

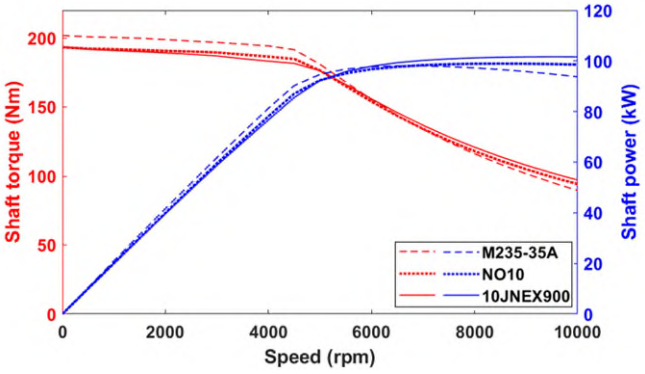

(b)

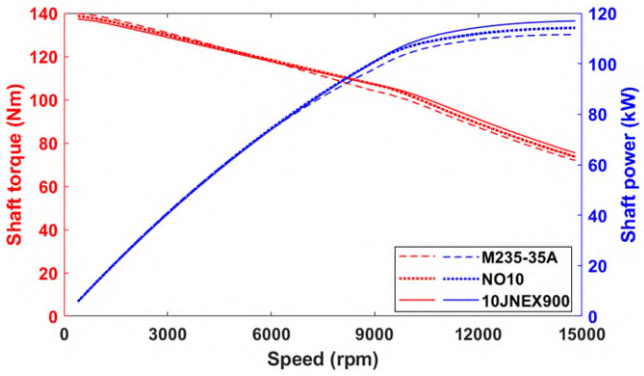

(c)

Fig. 10 Continuous thermal envelopes (torque-speed and power-speed) of the three motors with maximum temperature inputs: magnet = 140℃, stator winding = 160℃, rotor winding = 200℃. (a) PMa-SynRM, (b) IPM, and (c) IM.

Fig. 11 shows the mechanical stress and radial displacement of the IPM of Nissan Leaf traction system at a 20% over the maximum speed of 10000 rpm. The maximum rotor stress is about 418 MPa with M235-35A and NO10, while it is 410 MPa with 10JNEX900. The average rotor stress across the bridge between outer layer magnet and rotor outer surface are listed in TABLE II, as well as the maximum rotor displacement in radial direction. The IPM with both M235-35A and 10JNEX900 laminations can safely operate at the 20% over rotor maximum speed, and further away from the safety margin, while the maximum rotor stress is higher than material yield stress in small regions with NO10 (see Fig. 11a) , requiring possibly to improve the mechanical design.

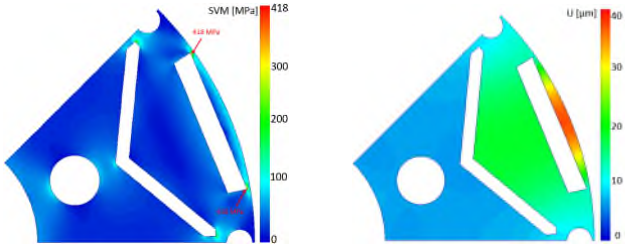

(a) (b)

Fig. 11 Mechanical performance of the IPM with NO10 at a 20% over the maximum speed 10000 r/min. (a) Von Mises stress (SVM), (b) radial displacement.

TABLE II
MECHANICAL PERFORMANCE OF THE IPM

	M235-35A	NO10	JFE
Yield stress (MPa)	460	370	604
Young's modulus (GPa)	185	193	200
Average rotor stress across the bridge (MPa)	171	171	170
Maximum rotor displacement (μm)	39	38	37

V. CONCLUSION

The impact of e-steel grades on motor performance have been investigated in terms of on-load flux densities, torque-speed characteristics, iron losses, efficiency map, continuous torque envelope, as well as mechanical performance at a 20% over speed. Both 3% and 6.5 % Si-Fe as well as conventional laminations have been adopted in the IPM, PMa-SynRM and IM for traction systems.

From the perspective of electromagnetic performance, 6.5% Si-Fe has the advantages to produce a higher maximum motor efficiency and a better flux weakening capability for all investigated motors. In addition, it has significantly lower iron losses at frequency higher than 400Hz. However, 3% or lower silicon content lamination is a better option for low frequency performance. Furthermore, the 10JNEX900 is the best choice for high-speed motor design due to its inherent high yield stress. In addition, NO10 is probably not suitable for high-speed motor due to low mechanical strength. Therefore, selection of the most appropriate e-steel grade relies on different drive cycle analysis where low- and high-speed performances are compromised. A more expensive material may provide value for money in terms of performance such as a higher efficiency, which then leads to a reduced battery pack cost at a given vehicle range. Future work will introduce optimization of the designs with material grade selection as well as the influence on the cost.

VI. ACKNOWLEDGMENT

The authors gratefully acknowledge the support from the UK EPSRC FEMM Hub via a feasibility grant (EP/S018034/1). The data that supports these investigations are available from the corresponding author X. Y. Ma upon reasonable request, with the permission of Motor Design Limited (an Ansys company), since the IM and IPM motors are parts of their tutorials and the software material database was used. The PMa-SynRM motor model was created from reference [18].

REFERENCES

[1] Z. Q. Zhu, W. Q. Chu and Y. Guan, "Quantitative comparison of electromagnetic performance of electrical machines for HEVs/EVs," *CES Trans. Electr. Mach. and Syst.,* vol. 1, no. 1, pp. 37-47, Mar. 2017.

[2] C. Chan, "The state of the art of electric and hybrid vehicles," *Proceedings of the IEEE,* vol. 90, no. 2, pp. 247-275, Feb. 2002.

[3] N. Bianchi, S. Bolognani, D. Bon and M. D. Pre, "Rotor flux-barrier design for torque ripple reduction in synchronous reluctance and PM-assisted synchronous reluctance motors," *IEEE Trans. Ind. appl.,* vol. 45, no. 3, pp. 921-928, May/Jun. 2009.

[4] X. Chen, J. Wang, P. Lazari and L. Chen, "Permanent magnet assisted synchronous reluctance machine with fractional-slot winding configurations," in *IEMDC*, Chicago, IL, USA, pp. 374-381, 12-15 May 2013.

[5] A. Krings, M. Cossale, A. Tenconi, J. Soulard, A. Cavagnino and A. Boglietti, "Characteristics comparison and selection guide for magnetic materials used in electrical machines," in *IEMDC*, Coeur d'Alene, ID, USA, pp. 1152-1157, 10-13 May 2015.

[6] H. Haiji, K. Okada, T. Hiratani, M. Abe and M. Ninomiya, "Magnetic properties and workability of 6.5% Si steel sheet," *J. Magn. Magn. Mater.,* vol. 160, pp. 109-114, 1996.

[7] J. J. H. Paulides, G. W. Jewell and D. Howe, "An evaluation of alternative stator lamination materials for a high-speed, 1.5 MW, permanent magnet generator," *IEEE Trans. Magn.,* vol. 40, no. 4, pp. 2041-2043, Jul. 2004.

[8] N. Fernando, G. Vakil, P. Arumugam, E. Amankwah, C. Gerada and S. Bozhko, "Impact of soft magnetic material on design of high-speed permanent-magnet machines," *IEEE Trans. Ind. Electron.,* vol. 64, no. 3, pp. 2415-2423, Mar. 2017.

[9] D. J. Powell, G. W. Jewell, S. D. Calverley and D. Howe, "Iron loss in a modular rotor switched reluctance machine for the 'more-electric' areo-engine," *IEEE Trans. Magn.,* vol. 41, no. 10, pp. 3934-3936, Oct. 2005.

[10] H. Sobur, K. Kiyota and A. Chiba, "Parameter identification for acoustic noise analysis of SRM made of 6.5% Si steel and amorphous iron-comparison of noise analysis and experiment," in *23rd ICEMs*, Hamamatsu, Japan, 24-27 Nov. 2020.

[11] G. Ouyang, X. Chen, Y. Liang, C. Macziewski and J. Cui, "Review of Fe-6.5 wt% Si high silicon steel- a promising soft magnetic material for sub-kHz application," *J. Magn. Magn. Mater.,* vol. 481, pp. 234-250, Feb. 2019.

[12] G. Bertotti, "General properties of power losses in soft ferromagnetic materials," *IEEE Trans. Magn.,* vol. 24, no. 1, pp. 621-630, Jan 1988.

[13] "49% Cobalt-Iron-Alloys," VAC, [Online]. Available: https://www.vacuumschmelze.com/products/soft-magnetic-materials-and-stamped-parts/49-Cobalt-Iron---VACOFLUX-and-VACODUR. [Accessed 12 Feb 2022].

[14] M. Miyazaki, M. Ichikawa, T. Komatsu and K. Matusita, "Formation and electronic state of Do3-type ordered structure in sputtered Fe-Si thin-films," *J. Appl. Pyhs.,* vol. 71, no. 5, pp. 2368-2374, 1992.

[15] M. Popescu and N. Riviere, "Electrical steel and motors performances, role of lamination thickness," in *WMM20*, Rome, Italy, pp. 1-27, 3-5 Nov 2020.

[16] C. K. Hou, "Effect of silicon on the loss separation and permeability of laminated steels," *J. Magn. Magn. Mater.,* vol. 26, no. 1, pp. 280-290, 1996.

[17] "Motor-CAD software," Motor design limited, [Online]. Available: https://www.motor-design.com/motor-cad/. [Accessed 15 Jul. 2021].

[18] A. Walker, M. Galea, D. Gerada, C. Gerada, A. Mebarki and N. Brown, "Development and design of a high performance traction machine for the FreedomCar 2020 traction machine targets," in *XXII ICEM*, Lausanne, Switzerland, pp. 1611-1617, 4-7 Sept. 2016.

BIOGRAPHIES

X. Y. Ma received her B.Eng. degree and PhD degree in Electrical Engineering from The University of Sheffield, U.K., in 2012 and 2018, respectively and her M.Sc. degree in sustainable energy systems from The University of Edinburgh, U.K., in 2013.

She joined the Warwick Manufacturing Group (WMG), University of Warwick, Coventry, U.K., in 2018, as a Research Fellow in Electric Machines. Her research activities are focused on design and modelling of switched reluctance machines, synchronous reluctance machines as well as PM machines, including impact of manufacturing on machine performance.

J. Soulard (M'00) received her PhD degree in Electrical Engineering from University of Paris VI, France in 1998.

She carried out academic research at KTH Royal Institute of Technology in Stockholm, Sweden until 2016, involving design and development of e-machines for renewable energy generation, industrial drives and electrified transport systems, with the Swedish industry. She is currently Associate Professor in Electric Machines at WMG. Her research activities are focused on impact of manufacturing on electric machine performance, with the aim to improve understanding and modelling approaches suitable at all stages of e-machine development.

C. Slater completed his PhD at the University of Birmingham in 2011 where he remained as a research fellow until 2016. Dr Slater moved to Warwick in 2016 and helped with the design and build of the new Advanced Materials and Manufacturing Centre, home to the Advanced Steel Research Centre as a senior research fellow. Dr Slater manages the rapid alloy production suite. His main areas of research are in the fields of alloy development as well as net shape casting and forging.

C. Davis is a Fellow of the Institute of Materials, Minerals and Mining and currently holds a RAEng / Tata Steel Chair in Low Energy Steel Processing. She completed her PhD in Metallurgy at the University of Cambridge, sponsored by British Steel and then held College and SERC fellowships.

She worked briefly as a lecturer at the University of Cambridge, before moving to the University of Birmingham, initially as a lecturer before promotions to senior lecturer, reader then professor. She moved to WMG, University of Warwick in 2014 and now leads the Advanced Steel Research Centre. Her area of research is the relationship between processing-microstructure-properties in steels and electromagnetic sensors for steel microstructure evaluation.